

Light-emitting nanostructures formed by intense, ultrafast electronic excitation in silicon (100)

Alex V. Hamza,^{a)} Micheal W. Newman, Peter A. Thielen, Howard W. H. Lee, Thomas Schenkel, Joseph W. McDonald, and Dieter H. Schneider
Lawrence Livermore National Laboratory, University of California, Livermore, California 94551

(Received 1 May 2001; accepted for publication 20 August 2001)

The intense, ultrafast electronic excitation of clean silicon (100)-(2×1) surfaces leads to the formation of silicon nanostructures embedded in silicon, which photoluminescence at ~560 nm wavelength (~2 eV band gap). The silicon surfaces were irradiated with slow, highly charged ions (e.g., Xe⁴⁴⁺ and Au⁵³⁺) to produce the electronic excitation. The observation of excitonic features in the luminescence is particularly unusual for silicon nanostructures. The temperature dependence and the measurement of the triplet-singlet splitting of the emission strongly support the excitonic assignment. © 2001 American Institute of Physics. [DOI: 10.1063/1.1413958]

The deposition of potential energy from slow, highly charged ions (SHCI) in semiconductor surfaces forms highly localized regions of intense electronic excitation^{1,2} on femto-second time scales.³ The relaxation of the intense electronic excitation leads to motion of the atoms in the surface, which can freeze into metastable geometric structures with different electronic properties. Slow, highly charged ions provide their electronic excitation in a nanometer-sized volume. In this letter, we report on the photoluminescence observed from the nanometer-sized defects in silicon surfaces produced by slow, highly charged ions.

Samples of float-zone silicon (100) were heated to 1300 K in ultrahigh vacuum (base pressure <5×10⁻¹⁰ Torr) to produce a clean surface exhibiting a (2×1) low-energy electron diffraction pattern. Secondary ion mass spectroscopy with highly charged ions was performed to ensure complete removal of the native oxide layer and any surface contaminants. The samples were then irradiated at normal incidence with slow, highly charged ions extracted from the electron-beam ion trap.⁴ Secondary electrons emitted from individual ion impacts were detected with an annular microchannel plate to monitor the total ion dose with high efficiency (~100%).⁵ After exposure, the samples were removed from vacuum and transferred to the photoluminescence chamber.

Atomic-force microscopy images revealed the formation of craters at individual slow, highly charged ion impact sites. The craters were ~15 nm in diameter for Xe⁴⁴⁺. For Xe⁴⁴⁺ impacts, the number of removed silicon atoms was ~100/ion as measured by catching the removed atoms on a diamond-like carbon surface which was subsequently analyzed by heavy-ion backscattering (see Ref. 2 for a description of the technique).

Photoluminescence (PL) measurements were performed using the doubled output from a femtosecond Ti-sapphire laser and a variable emission optical parametric amplifier as the excitation source. The luminescence was collected using a scanning monochromator with holographic grating. A photomultiplier tube was used for photon detection using a lock-in amplifier for signal processing. All samples were re-

introduced into vacuum (<10⁻³ Torr) prior to the photoluminescence measurements.

Photoluminescence spectra were taken from both SHCI exposed and unexposed regions on each sample. No effect on the photoluminescence signal was observed with variation of the kinetic energy of the ions from 50 to 700 keV. A threshold was observed for the electronic excitation. Ions with potential energy less than ~10 keV/ion (Xe²³⁺) produced no photoluminescence signal. The photoluminescence signal was linearly proportional to the potential energy carried by the ion up to ~130 keV/ion (Au⁶³⁺) once the 10 keV/ion threshold was reached. Figure 1 shows the photoluminescence spectrum from the irradiated and unirradiated areas of the silicon (100) sample. Irradiation conditions were 2×10¹¹ Xe⁴⁴⁺/cm² at 616 keV kinetic energy for Fig. 1. The laser excitation wavelength was 379 nm. The PL from the irradiated area is characterized by a series of relatively narrow emission lines. No other visible luminescence was ob-

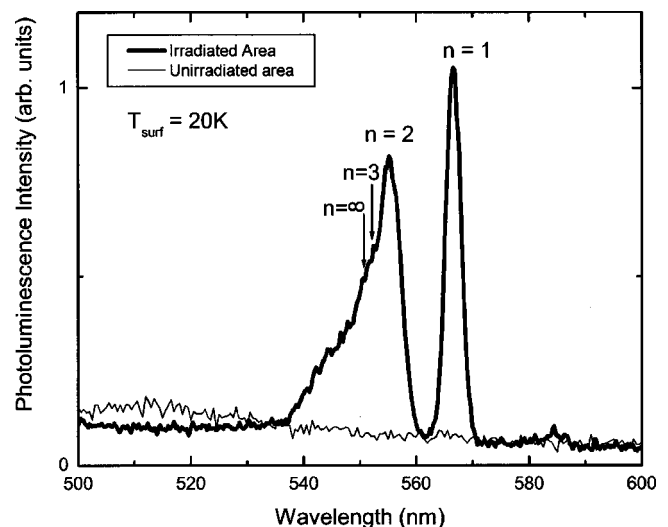


FIG. 1. Photoluminescence at 20 K from float-zone Si(100) irradiated with 2×10¹¹ Xe⁴⁴⁺/cm² and from unirradiated Si(100). The laser excitation wavelength was 379 nm (3.27 eV). The *n*=1 exciton is at 566 nm and the *n*=2 exciton is at 555 nm. Also labeled are the positions of the *n*=3 and series limit (*n*=∞) excitons.

^{a)}Electronic mail: hamza1@llnl.gov

served. The dashed line represents the luminescence signal from the unirradiated area. No features were observed in the visible range on the unirradiated area, as was true of “as-received” wafers.

The PL signal increased linearly by a factor of ~ 8 with the Xe^{40+} dose (irradiance) from 1×10^{10} to $2 \times 10^{11}/\text{cm}^2$. Above 2×10^{11} to $1 \times 10^{12}/\text{cm}^2$ the PL intensity increased by only a factor of ~ 2 . A dose of $\sim 2 \times 10^{11}/\text{cm}^2$ is the irradiance where overlap of impact sites begins, indicating that the impact sites have a diameter of ~ 15 nm, in agreement with the atomic-force microscope measurements. The linear dependence of the PL intensity on dose also confirms the PL comes from the individual impact sites.

The PL observed in Fig. 1 from the irradiated area is well above the band gap of bulk crystalline silicon (1.17 eV). The features of the PL suggest that the emission results from the radiative recombination of a photogenerated exciton localized within the individual SHCI impact sites. The energy spacing of the luminescence peaks is that of a hydrogenic series given by $E_N = E_0 - \alpha/n$; where n is the principal quantum number, E_0 is the direct interband transition, and α is the exciton binding energy. Only the $n=1$ and $n=2$ states are clearly resolved. The band-gap energy of this exciton is much higher than that of bulk silicon. Thus, a barrier must exist that keeps the exciton confined to the higher band-gap region. Since the samples are removed from vacuum and reintroduced to vacuum for PL measurements, the native oxide of silicon may provide such a barrier.

An alternative explanation for the origin of the luminescence is trap states inside the thin oxide layer that forms over the irradiated surface. The luminescence features are rapidly quenched during photoexcitation in air. This is attributed to an enhanced growth of the surface oxide into the substrate due to the laser exposure. If the luminescence were due to a trap state in the oxide, the trap state must be some structure, which is formed by an intense, ultrafast electronic excitation and then subsequently oxidized. However, the dispersion of the luminescence argues against such a trap state.

The exciton dispersion is evidenced by the square-root dependence of the energy loss (the laser excitation energy less the luminescence energy) on the laser excitation energy. If the exciton were thermalized at the bottom of its dispersion curve, the luminescence energy would be independent of the laser excitation energy as long as the laser energy is larger than the luminescent energy. The observed dispersion is due to an incomplete thermalization of the exciton. The exciton dispersion relationship will be discussed in more detail in a subsequent publication.

The temperature dependence of the visible photoluminescence from SHCI-irradiated silicon has also been investigated for a high dose ($1 \times 10^{12}/\text{cm}^2$) Xe^{44+} -irradiated Si(100)-(2 \times 1) sample. The sample was mounted in vacuum to a closed-cycle He cryostat and cooled to 17 K. PL measurements were taken at 30 K intervals up to 395 K. The PL spectrum showed no shifts or broadening in this temperature range. The PL intensity increased by a factor of ~ 2 by increasing the sample temperature from 17 to 190 K. Above 190 K the PL signal decreases with temperature.

The observed temperature dependence can be explained by considering the electron-hole exchange splitting. Both

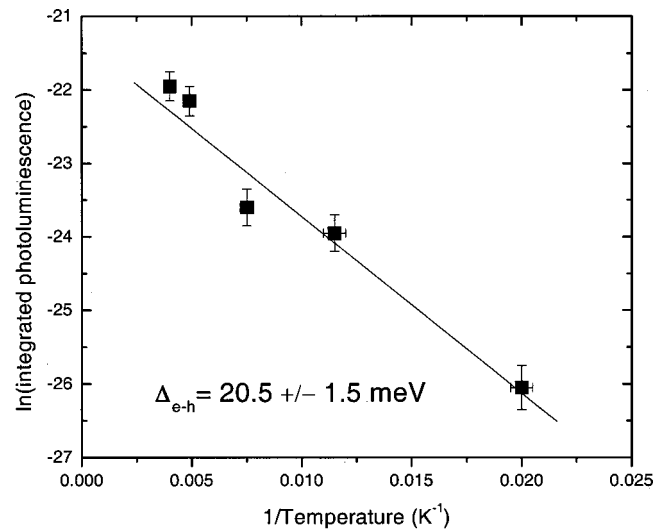


FIG. 2. Arrhenius plot of the integrated photoluminescence intensity for the $n=1$ exciton feature for Xe^{40+} -irradiated float-zone Si(100) vs inverse temperature. The solid line is the least-squares fit of the data to Eq. (1).

the electron and the hole in the exciton have spin $\frac{1}{2}$. Thus, the exciton state is split by the exchange interaction (Δ) into a spin singlet and a spin triplet, with the spin triplet lower in energy.⁶ Excitons are predominantly created in the nonradiative triplet state because the absorption is inversely proportional to the radiative lifetime. The radiative decay rate of the singlet is 400–1200 times faster than the triplet radiative decay rate.⁷ In order to observe radiative decay (luminescence) the initially populated triplet will be converted to the singlet via thermal energy. The population of the singlet can be written as

$$N_s = N_t \exp(-\Delta/kt), \quad (1)$$

where N_s and N_t are the occupation numbers for the spin singlet and spin triplet, respectively.

Figure 2 shows an Arrhenius plot of the integrated intensity of the $n=1$ exciton level versus the inverse sample temperature. By fitting Eq. (1) to the data in Fig. 2, an electron-hole exchange energy of 20 meV is obtained. This value is dramatically larger than the exchange splitting for the free exciton in bulk crystalline silicon ($\Delta < 0.15$ meV).⁸ Similar electron-hole exchange energies have been reported for porous silicon⁷ and silicon nanocrystals in silica.⁹ Thus, the temperature dependence of the photoluminescence indicates the origin of the emission is from an exciton in the nanometer-sized silicon structure.

The intense, ultrafast electronic excitation that results from the deposition of potential energy from slow, highly charged ion impacts on silicon (100) surfaces leads to the formation of nanometer-sized structures. Photogenerated excitons within these regions radiatively decay, emitting ~ 2 eV light.

This work was performed under the auspices of the U.S. Department of Energy by the University of California, Lawrence Livermore National Laboratory, under Contract No. W-7405-ENG-48 and was supported by the Division of Chemical Sciences of the Office of Science.

- ¹T. Schenkel, A. V. Hamza, A. V. Barnes, D. H. Schneider, J. C. Banks, and B. L. Doyle, *Phys. Rev. Lett.* **81**, 2590 (1998).
- ²T. Schenkel, A. V. Barnes, T. R. Niedermayr, M. Hattass, M. W. Newman, G. A. Machicoane, J. W. McDonald, A. V. Hamza, and D. H. Schneider, *Phys. Rev. Lett.* **83**, 4273 (1999).
- ³M. Hattass, T. Schenkel, A. V. Hamza, A. V. Barnes, M. W. Newman, J. W. McDonald, T. R. Niedermayr, G. A. Machicoane, and D. H. Schneider, *Phys. Rev. Lett.* **82**, 4795 (1999).
- ⁴D. H. Schneider and M. A. Briere, *Phys. Scr.* **53**, 228 (1996).
- ⁵T. Schenkel, A. V. Barnes, A. V. Hamza, and D. H. Schneider, *Eur. Phys. J. D* **1**, 297 (1998).
- ⁶C. H. Henery, R. A. Faulkner, and K. Nassua, *Phys. Rev.* **183**, 789 (1969).
- ⁷P. D. J. Calcott, K. J. Nash, L. T. Kane, and D. Brumhead, *J. Phys.: Condens. Matter* **5**, L91 (1993).
- ⁸J. C. Merl, M. Capizi, P. Fiorini, and A. Frova, *Phys. Rev. B* **17**, 4821 (1978).
- ⁹M. L. Brongersma, P. G. Kik, A. Polman, K. S. Min, and H. A. Atwater, *Appl. Phys. Lett.* **76**, 351 (2000).